

Narrow Escape, Part III: Non-Smooth Domains and Riemann Surfaces

A. Singer,¹ Z. Schuss,² and D. Holcman³

Received January 26, 2005; accepted August 19, 2005; Published Online: January 20, 2006

We consider the narrow escape problem in two-dimensional Riemannian manifolds (with a metric g) with corners and cusps, in an annulus, and on a sphere. Specifically, we calculate the mean time it takes a Brownian particle diffusing in a domain Ω to reach an absorbing window when the ratio $\varepsilon = \frac{|\partial\Omega_a|_g}{|\partial\Omega|_g}$ between the absorbing window and the otherwise reflecting boundary is small. If the boundary is smooth, as in the cases of the annulus and the sphere, the leading term in the expansion is the same as that given in part I of the present series of papers, however, when it is not smooth, the leading order term is different. If the absorbing window is located at a corner of angle α , then $E\tau = \frac{|\Omega|_g}{\alpha D} [\log \frac{1}{\varepsilon} + O(1)]$, if near a cusp, then $E\tau$ grows algebraically, rather than logarithmically. Thus, in the domain bounded between two tangent circles, the expected lifetime is $E\tau = \frac{|\Omega|}{(d-1)D} (\frac{1}{\varepsilon} + O(1))$, where $d < 1$ is the ratio of the radii. For the smooth boundary case, we calculate the next term of the expansion for the annulus and the sphere. It can also be evaluated for domains that can be mapped conformally onto an annulus. This term is needed in real life applications, such as trafficking of receptors on neuronal spines, because $\log \frac{1}{\varepsilon}$ is not necessarily large, even when $\varepsilon = \frac{|\partial\Omega_a|_g}{|\partial\Omega|_g}$ is small. In these two problems there are additional parameters that can be small, such as the ratio δ of the radii of the annulus. The contributions of these parameters to the expansion of the mean escape time are also logarithmic. In the case of the annulus the mean escape time is $E\tau = \frac{|\Omega|_g}{\pi D} [\log \frac{1}{\varepsilon} + \frac{1}{2} \log \frac{1}{\delta} + O(1)]$.

KEY WORDS: Brownian motion on Riemannian manifolds; Exit problem; Singular perturbations.

¹ Department of Mathematics, Yale University, 10 Hillhouse Ave. PO Box 208283, New Haven, CT 06520-8283, USA; e-mail: amit.singer@yale.edu

² Department of Mathematics, Tel-Aviv University, Tel-Aviv 69978, Israel, e-mail: schuss@post.tau.ac.il

³ Department of Mathematics, Weizmann Institute of Science, Rehovot 76100 Israel, e-mail: holcman@wisdom.weizmann.ac.il

1. INTRODUCTION

In many applications it is necessary to find the mean first passage time (MFPT) of a Brownian particle to a small absorbing window in the otherwise reflecting boundary of a given bounded domain. This is the case, for example, in the permeation of ions through protein channels of cell membranes,⁽¹⁾ and in the trafficking of AMPA receptors on nerve cell membranes.^(2,3) While the first example is three dimensional the second is two dimensional, which leads to very different results. In this paper we consider the two dimensional case.

In the first two parts ^(4,5) of this series of papers, we derived an asymptotic expansion of the mean time a Brownian particle takes to reach a small absorbing window $\partial\Omega_a$ in the otherwise reflecting boundary $\partial\Omega$ of a given domain Ω in two and three dimensions. In particular, we found that if Ω is a two-dimensional Riemannian surface with smooth boundary, the leading term in the asymptotic expansion for $\varepsilon = \frac{|\partial\Omega_a|_g}{|\partial\Omega|_g} \ll 1$ is

$$E\tau = \frac{|\Omega|_g}{\pi D} \left[\log \frac{1}{\varepsilon} + O(1) \right]. \tag{1.1}$$

We show here that if the boundary contains corners or cusps, the leading order term in the expansion is not the same as that in the case of smooth boundaries. When the absorbing arc is located at a corner of angle α , the MFPT is

$$E\tau = \frac{|\Omega|_g}{D\alpha} \left[\log \frac{1}{\varepsilon} + O(1) \right]. \tag{1.2}$$

For example, the MFPT from a rectangle with sides a and b to an absorbing window of size ε at the corner ($\alpha = \pi/2$, see Fig. 1), is

$$E\tau = \frac{2|\Omega|}{D\pi} \left[\log \frac{a}{\varepsilon} + \log \frac{2}{\pi} + \frac{\pi}{6} \frac{b}{a} + 2\beta^2 + O\left(\frac{\varepsilon}{a}, \beta^4\right) \right],$$

where $|\Omega| = ab$ and $\beta = e^{-\pi b/a}$. The calculation of the second order term turns out to be similar to that in the annulus case. The pre-logarithmic factor $\frac{|\Omega|_g}{D\alpha}$ is the result of the different singularity of the Neumann function at the corner. It can be obtained by either the method of images, or by the conformal mapping $z \mapsto z^{\pi/\alpha}$ that flattens the corner. In the vicinity of a cusp $\alpha \rightarrow 0$, therefore the asymptotic expansion (1.2) is invalid. We find that near a cusp the MFPT grows algebraically fast as $\frac{1}{\varepsilon^\lambda}$, where λ is the order of the cusp. Note that the MFPT grows faster to infinity as the boundary is more singular. The change of behavior from a logarithmic growth to an algebraic one expresses the fact that entering a cusp is a rare Brownian event. For example, the MFPT from the domain bounded between two tangent circles to a small arc at the common point

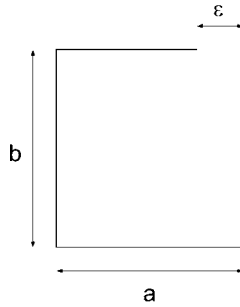


Fig. 1. Rectangle of sizes a and b with a small absorbing segment of size ϵ at the corner.

(see Fig. 3) is

$$E\tau = \frac{|\Omega|}{(d^{-1} - 1)D} \left(\frac{1}{\epsilon} + O(1) \right),$$

where $d < 1$ is the ratio of the radii. This result is obtained by mapping the cusped domain conformally onto the upper half plane. The singularity of the Neumann function is transformed as well. The leading order term of the asymptotics can be found for any domain that can be mapped conformally to the upper half plane.

In three dimensions the class of isolated singularities of the boundary is much richer than in the plane. The results of Ref. 4 cannot be generalized in a straightforward way to windows located near a singular point or arc of the boundary. We postpone the investigation of the MFPT to windows at isolated singular points in three dimensions to a future paper.

While the second term in the asymptotic expansion of the MFPT in three dimensions is much smaller than the first one, it is not necessarily so in two dimensions, because of the slow growth of the logarithmic function. It is necessary, therefore, to find the second term in the expansion in the two-dimensional case. This term was found for the case of a planar circular disk in Ref. 5, and can therefore be found for all simply connected domains in the plane that can be mapped conformally onto the disk. Similarly, it can be found for simply connected domains on two-dimensional Riemannian manifolds that can be mapped conformally on the planar disk. For example, the sphere with a circular cap cut off can be projected stereographically onto the disk, and so the second term for the narrow escape problem for such domains can be found.

Next, we consider narrow escape from an annulus, whose boundary is reflecting, except for a small absorbing arc on the inner circle. Specifically, the annulus is the domain $R_1 < r < R_2$, with all reflecting boundaries except for a small absorbing window located at the inner circle (see Fig. 4). The inversion $w = 1/z$ transforms this case into that of the absorbing boundary on the outer circle. Setting $\beta = \frac{R_1}{R_2} < 1$, the MFPT, averaged with respect to a uniform initial distribution,

can be written as

$$E\tau = \frac{(R_2^2 - R_1^2)}{D} \left[\log \frac{1}{\varepsilon} + \log 2 + 2\beta^2 \right] + \frac{1}{D} \left[\frac{1}{2} \frac{R_2^2}{1 - \beta^2} \log \frac{1}{\beta} - \frac{1}{4} R_2^2 + O(\varepsilon, \beta^4) R_2^2 \right]. \quad (1.3)$$

The ε contribution belongs to a singular perturbation problem with a boundary layer solution and an almost constant outer solution with singular fluxes near the edges of the window, whereas the β contribution is just the singularity of Green's function at the origin—a problem with a regular flux. Note that Eq. (1.3) contains two terms of the asymptotic expansion of $E\tau$. This result is generalized to a sphere with two antipodal circular caps removed. We find that for $\beta \ll 1$ the maximum exit time is attained near the south pole, as expected. This result can be generalized to manifolds that can be mapped conformally onto the given domain. The calculation of the second term involves the solution of the mixed Dirichlet-Neumann problem for harmonic functions in Ω . While in the three dimensional case this is a classical problem in mechanics, diffusion, elasticity theory, hydrodynamics, and electrostatics^(6–8), the two dimensional problem did not draw as much attention in the literature.

We also calculate the second term in the asymptotic expansion for the 2-sphere $x^2 + y^2 + z^2 = R^2$. The calculation is made possible by the stereographic projection that maps the Riemann sphere onto a circular disk, a problem that was solved in Ref. 5. The boundary in this case is a spherical cap of central angle δ at the north pole, where ε is the ratio between the absorbing arc and the entire boundary circle. We find that the MFPT, averaged with respect to an initial uniform distribution, is given by

$$E\tau = \frac{|\Omega|_g}{2\pi D} \left[\log \frac{1}{\delta} + 2 \log \frac{1}{\varepsilon} + 3 \log 2 - \frac{1}{2} + O(\varepsilon, \delta^2 \log \delta, \delta^2 \log \varepsilon) \right], \quad (1.4)$$

where $|\Omega|_g = 4\pi R^2$ is the surface area of the sphere. Note that there are two small parameters that control the behavior of the MFPT in this problem. The small ε contributes as Eq. (1.1) predicts, whereas the small δ parameter contributes only a half of the logarithm.

The analysis of Brownian motion near corners and cusps assumes point particles. However, if the Brownian particle has a finite volume, the effective contact boundary between the particle and the boundary of the domain has neither corners nor cusps. This fact, though, does not change the asymptotic expansion of the MFPT as long as the radius of the particle is much smaller than the size of the window. This is due to the change in the singularity of the Neumann function from logarithmic to algebraic along the boundary near the singular point. If the size of the particle is smaller than the transition region from one singularity of

the Neumann function to the other, the MFPT will be the same as that of a point particle.

As a possible application of the present results, we mention the calculation of the diffusion coefficient from the statistics of the lifetime of a receptor in a corral on the surface of a neuronal spine.⁽³⁾

2. DOMAINS WITH CORNERS

Consider a Brownian motion in a rectangle $\Omega = (0, a) \times (0, b)$ of area ab . The boundary is reflecting except the small absorbing segment $\partial\Omega_a = [a - \varepsilon, a] \times \{b\}$ (see Fig. 1). The MFPT $v(x, y)$ satisfies the boundary value problem

$$\begin{aligned} \Delta v &= -1, & (x, y) \in \Omega, \\ v &= 0, & (x, y) \in \partial\Omega_a, \\ \frac{\partial v}{\partial n} &= 0, & (x, y) \in \partial\Omega - \partial\Omega_a. \end{aligned} \tag{2.1}$$

The function $f = \frac{b^2 - y^2}{2}$ satisfies

$$\begin{aligned} \Delta f &= -1, & (x, y) \in \Omega, \\ f &= 0, & (x, y) \in \partial\Omega_a, \\ \frac{\partial f}{\partial n} &= 0, & (x, y) \in \{0\} \times [0, b] \cup \{a\} \times [0, b] \cup [0, a] \times \{0\}, \\ \frac{\partial f}{\partial n} &= -b, & (x, y) \in [0, a - \varepsilon] \times \{b\}, \end{aligned} \tag{2.2}$$

therefore, the function $u = v - f$ satisfies

$$\begin{aligned} \Delta u &= 0, & (x, y) \in \Omega, \\ u &= 0, & (x, y) \in \partial\Omega_a, \\ \frac{\partial u}{\partial n} &= 0, & (x, y) \in \{0\} \times [0, b] \cup \{a\} \times [0, b] \cup [0, a] \times \{0\}, \\ \frac{\partial u}{\partial n} &= b, & (x, y) \in [0, a - \varepsilon] \times \{b\}. \end{aligned} \tag{2.3}$$

A solution for u in the form of separation of variables is

$$u(x, y) = \frac{a_0}{2} + \sum_{n=1}^{\infty} a_n \cosh \frac{\pi n y}{a} \cos \frac{\pi n x}{a}, \tag{2.4}$$

where the coefficients a_n are to be determined by the boundary conditions at $y = b$

$$u(x, b) = \frac{a_0}{2} + \sum_{n=1}^{\infty} a_n \cosh \frac{\pi nb}{a} \cos \frac{\pi nx}{a} = 0, \quad x \in (a - \varepsilon, a), \tag{2.5}$$

$$\frac{\partial u}{\partial y}(x, b) = \frac{\pi}{a} \sum_{n=1}^{\infty} n a_n \sinh \frac{\pi nb}{a} \cos \frac{\pi nx}{a} = b, \quad x \in (0, a - \varepsilon).$$

Setting $c_n = a_n \sinh \frac{\pi nb}{a}$, we have

$$\begin{aligned} \frac{c_0}{2} + \sum_{n=1}^{\infty} \frac{c_n}{1 + H_n} \cos n\theta &= 0, \quad \pi - \delta < \theta < \pi, \\ \sum_{n=1}^{\infty} n c_n \cos n\theta &= \frac{ab}{\pi}, \quad 0 < \theta < \pi - \delta, \end{aligned} \tag{2.6}$$

where $\delta = \frac{\pi\varepsilon}{a}$ and $H_n = \tanh(\frac{\pi nb}{a}) - 1, n \geq 1$. Note that $H_n = O(\beta^{2n})$ for $\beta = \exp\{-\frac{\pi b}{a}\} < 1$. The rectangle problem and annulus problem (Eq. (4.10)) are almost mathematically equivalent, and Eq. (4.27) gives the value of c_0

$$\begin{aligned} c_0 &= \frac{2ab}{\pi} \left[2 \log \frac{1}{\delta} + 2 \log 2 + 4\beta^2 + O(\delta, \beta^4) \right] \\ &= \frac{4ab}{\pi} \left[\log \frac{a}{\varepsilon} + \log \frac{2}{\pi} + 2\beta^2 + O\left(\frac{\varepsilon}{a}, \beta^4\right) \right]. \end{aligned} \tag{2.7}$$

The error term due to $O(\beta^4)$ is generally small. For example, in a square $a = b$ and $\beta = e^{-\pi}$ so that $\beta^4 \approx 3 \times 10^{-6}$. The MFPT averaged with respect to a uniform initial distribution is

$$E\tau = \frac{c_0}{2} + \frac{b^2}{3} = \frac{2ab}{\pi} \left[\log \frac{a}{\varepsilon} + \log \frac{2}{\pi} + \frac{\pi b}{6a} + 2\beta^2 + O\left(\frac{\varepsilon}{a}, \beta^4\right) \right]. \tag{2.8}$$

The leading order term of the MFPT is

$$\frac{2|\Omega|}{\pi} \log \frac{a}{\varepsilon}, \tag{2.9}$$

which is twice as large than (4.29). The general result (1.1) was proved for a domain with smooth boundary (at least C^1). However, in the rectangle example, the small hole is located at the corner. The additional factor 2 is the result of the different singularity of the Neumann function at the corner, which is 4 times larger than that of the Green function. At the corner there are 3 image charges—the number of images that one sees when standing near two perpendicular mirror plates. In general, for a small hole located at a corner of an opening angle α (see

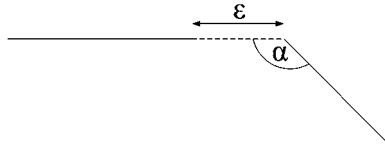


Fig. 2. A small opening near a corner of angle α .

Fig. 2), the MFPT is to leading order

$$E\tau = \frac{|\Omega|}{D\alpha} \left(\log \frac{1}{\epsilon} + O(1) \right). \tag{2.10}$$

This result is a consequence of the method of images for integer values of $\frac{\pi}{\alpha}$. For non-integer $\frac{\pi}{\alpha}$ we use the complex mapping $z \mapsto z^{\pi/\alpha}$ that flattens the corner. The upper half plane Neumann function $\frac{1}{\pi} \log z$ is mapped to $\frac{1}{\alpha} \log z$ and the analysis of Refs. [2, 4] gives (2.10).

To see that the area factor $|\Omega|$ remains unchanged under the conformal mapping $f : (x, y) \mapsto (u(x, y), v(x, y))$, we note that this factor is a consequence of the compatibility condition, that relates the area to the integral

$$\int_{\Omega} \Delta_{(x,y)} w \, dx \, dy = -\frac{|\Omega|}{D},$$

where $w(x, y) = E[\tau | x(0) = x, y(0) = y]$ satisfies $\Delta_{(x,y)} w = -1/D$. The Laplacian transforms according to

$$\Delta_{(x,y)} w = (u_x^2 + u_y^2) \Delta_{(u,v)} w,$$

by the Cauchy-Riemann equations and the Jacobian of the transformation is $J = u_x^2 + u_y^2$. Therefore,

$$\int_{\Omega} \Delta_{(x,y)} w \, dx \, dy = \int_{f(\Omega)} \Delta_{(u,v)} w \, du \, dv.$$

This means that the compatibility condition of Ref. 4 remains unchanged and gives the area of the original domain.

3. DOMAINS WITH CUSPS

Here we find the leading order term of the MFPT for small holes located near a cusp of the boundary. A cusp is a singular point of the boundary. As $\alpha = 0$ at the cusp, one expects to find a different asymptotic expansion than (2.10). As an example, consider the Brownian motion inside the domain bounded between the circles $(x - 1/2)^2 + y^2 = 1/4$ and $(x - 1/4)^2 + y^2 = 1/16$ (see Fig. 3). The conformal mapping $z \mapsto \exp\{\pi i(1/z - 1)\}$ maps this domain onto the upper half

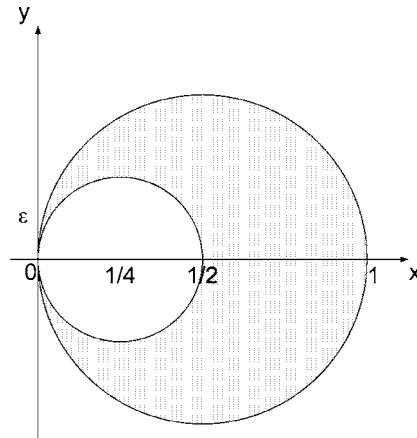


Fig. 3. The point (0, 0) is a cusp point of the dotted domain bounded between the two circles. The small absorbing arc of length ϵ is located at the cusp point.

plane. Therefore, the MFPT is to leading order

$$E\tau = \frac{|\Omega|}{D} \left(\frac{1}{\epsilon} + O(1) \right). \tag{3.1}$$

This result can also be obtained by mapping the cusped domain to the unit circle. The absorbing boundary is then transformed to an exponentially small arc of length $\exp\{-\pi/\epsilon\} + O(\exp\{-2\pi/\epsilon\})$, and Eq. (3.1) is recovered. If the ratio between the two radii is $d < 1$, then the conformal map that maps the domain between the two circles to the upper half plane is $\exp\{\frac{\pi i}{d^{-1}-1}(1/z - 1)\}$ (for $d = 1/2$ we arrive at the previous example), so the MFPT is to leading order

$$E\tau = \frac{|\Omega|}{(d^{-1} - 1)D} \left(\frac{1}{\epsilon} + O(1) \right). \tag{3.2}$$

The MFPT tends algebraically fast to infinity, much faster than the $O(\log \frac{1}{\epsilon})$ behavior near smooth or corner boundaries. The MFPT for a cusp is much larger because it is more difficult for the Brownian motion to enter the cusp than to enter a corner. The MFPT (3.2) can be written in terms of d instead of the area. Substituting $|\Omega| = \pi R^2(1 - d^2)$, we find

$$E\tau = \frac{\pi R^2 d(1 + d)}{D} \left(\frac{1}{\epsilon} + O(1) \right), \tag{3.3}$$

where R is the radius of the outer circle. Note that although the area of Ω is a monotonically decreasing function of d , the MFPT is a monotonically increasing function of d and tends to a finite limit as $d \rightarrow 1$.

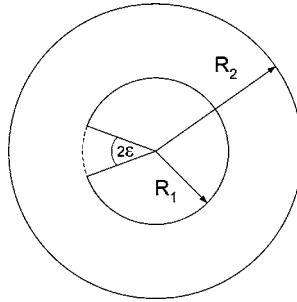


Fig. 4. An annulus $R_1 < r < R_2$. The particle is absorbed at an arc of length $2\varepsilon R_1$ (dashed line) at the inner circle. The solid lines indicate reflecting boundaries.

Similarly, one can consider different types of cusps and find that the leading order term for the MFPT is proportional to $1/\varepsilon^\lambda$, where λ is a parameter that describes the order of the cusp, and can be obtained by the same technique of conformal mapping.

4. THE ANNULUS

We consider a Brownian particle that is confined in the annulus $R_1 < r < R_2$. The particle can exit the annulus through a narrow opening of the inner circle (see Fig. 4). The MFPT $v(x)$ satisfies

$$\begin{aligned} \Delta v &= -1, \quad \text{for } R_1 < r < R_2, \\ \frac{\partial v}{\partial r} &= 0, \quad \text{for } r = R_2, \\ \frac{\partial v}{\partial r} &= 0, \quad \text{for } r = R_1, \quad |\theta - \pi| > \varepsilon, \\ v &= 0, \quad \text{for } r = R_1, \quad |\theta - \pi| < \varepsilon. \end{aligned} \tag{4.1}$$

The function $w = \frac{R_1^2 - r^2}{4}$ is a solution of the Dirichlet problem for Eq.(4.1) in the exterior domain of the inner circle $r > R_1$. More specifically, it satisfies the boundary value problem

$$\begin{aligned} \Delta w &= -1, \quad \text{for } R_1 < r < R_2, \\ \frac{\partial w}{\partial r} &= -\frac{1}{2}R_1, \quad \text{for } r = R_1, \\ \frac{\partial w}{\partial r} &= -\frac{1}{2}R_2, \quad \text{for } r = R_2, \\ w &= 0, \quad \text{for } r = R_1. \end{aligned} \tag{4.2}$$

The function $u = v - w$ satisfies

$$\begin{aligned} \Delta u &= 0, \quad \text{for } R_1 < r < R_2, \\ \frac{\partial u}{\partial r} &= \frac{1}{2}R_2, \quad \text{for } r = R_2, \\ \frac{\partial u}{\partial r} &= \frac{1}{2}R_1, \quad \text{for } r = R_1, \quad |\theta - \pi| > \varepsilon, \\ u &= 0, \quad \text{for } r = R_1, \quad |\theta - \pi| < \varepsilon. \end{aligned} \quad (4.3)$$

Separation of variables produces the solution

$$u(r, \theta) = \frac{a_0}{2} + \sum_{n=1}^{\infty} \left[a_n \left(\frac{r}{R_2} \right)^n + b_n \left(\frac{R_2}{r} \right)^n \right] \cos n\theta + \alpha \log \left(\frac{r}{R_1} \right), \quad (4.4)$$

where a_n , b_n and α are to be determined by the boundary conditions. Differentiating with respect to r yields

$$\frac{\partial u}{\partial r} = \sum_{n=1}^{\infty} n \left[\frac{a_n}{R_2} \left(\frac{r}{R_2} \right)^{n-1} - \frac{b_n R_2}{r^2} \left(\frac{R_2}{r} \right)^{n-1} \right] \cos n\theta + \frac{\alpha}{r}. \quad (4.5)$$

Setting $r = R_2$ gives

$$\frac{1}{2}R_2 = \frac{1}{R_2} \left[\sum_{n=1}^{\infty} n (a_n - b_n) \cos n\theta + \alpha \right], \quad (4.6)$$

therefore, $a_n = b_n$ and $\alpha = \frac{1}{2}R_2^2$, and we have

$$u(r, \theta) = \frac{a_0}{2} + \sum_{n=1}^{\infty} a_n \left[\left(\frac{r}{R_2} \right)^n + \left(\frac{R_2}{r} \right)^n \right] \cos n\theta + \frac{1}{2}R_2^2 \log \left(\frac{r}{R_1} \right). \quad (4.7)$$

The boundary conditions at $r = R_1$ become the dual series equations

$$\begin{aligned} \frac{a_0}{2} + \sum_{n=1}^{\infty} a_n \left[\left(\frac{R_2}{R_1} \right)^n + \left(\frac{R_1}{R_2} \right)^n \right] \cos n\theta &= 0, \quad \text{for } |\theta - \pi| < \varepsilon, \\ \sum_{n=1}^{\infty} n a_n \left[\left(\frac{R_2}{R_1} \right)^{n+1} - \left(\frac{R_1}{R_2} \right)^{n-1} \right] \cos n\theta &= \frac{R_2}{2R_1} (R_2^2 - R_1^2), \\ &\text{for } |\theta - \pi| > \varepsilon. \end{aligned}$$

Setting

$$c_n = \frac{R_1}{R_2} \left[\left(\frac{R_2}{R_1} \right)^{n+1} - \left(\frac{R_1}{R_2} \right)^{n-1} \right] a_n, \quad \text{for } n \geq 1, \quad (4.8)$$

and $c_0 = a_0$ converts the dual series equations to

$$\frac{c_0}{2} + \sum_{n=1}^{\infty} \frac{c_n}{1 + H_n} \cos n\theta = 0, \quad \text{for } \pi - \varepsilon < \theta < \pi, \tag{4.9}$$

$$\sum_{n=1}^{\infty} n c_n \cos n\theta = \frac{1}{2} (R_2^2 - R_1^2), \quad \text{for } 0 < \theta < \pi - \varepsilon, \tag{4.10}$$

where $H_n = -\frac{2\beta^{2n}}{1+\beta^{2n}}$ for $n \geq 1$, and $H_0 = 0$, with $\beta = \frac{R_1}{R_2} < 1$. Note that $H_n = O(\beta^{2n})$ which tends to zero exponentially fast (much faster than the n^{-1} decay required for the Collins method^(13,14), see also Ref. 4).

The case $H_n \equiv 0$ was solved in Ref. 5. We now try to find the correction of that result due to the non vanishing H_n . As in Ref. 5 the equation

$$\begin{aligned} \frac{c_0}{2} + \sum_{n=1}^{\infty} \frac{c_n}{1 + H_n} \cos n\theta = \\ \cos \frac{\theta}{2} \int_{\theta}^{\pi-\varepsilon} \frac{h_1(t) dt}{\sqrt{\cos \theta - \cos t}} \quad \text{for } 0 < \theta < \pi - \varepsilon \end{aligned}$$

defines the function $h_1(\theta)$ uniquely for $0 < \theta < \pi - \varepsilon$, the coefficients are given by

$$c_n = \frac{1 + H_n}{\sqrt{2}} \int_0^{\pi-\varepsilon} h_1(t) [P_n(\cos t) + P_{n-1}(\cos t)] dt, \tag{4.11}$$

and

$$c_0 = \sqrt{2} \int_0^{\pi-\varepsilon} h_1(t) dt. \tag{4.12}$$

Integrating equation (4.10) gives

$$\sum_{n=1}^{\infty} c_n \sin n\theta = \frac{1}{2} (R_2^2 - R_1^2) \theta, \quad \text{for } 0 < \theta < \pi - \varepsilon. \tag{4.13}$$

Substituting Eq. (4.13) in Eq. (4.11), changing the order of summation and integration, while using [Ref. 6, Eq. (2.6.31)],

$$\frac{1}{\sqrt{2}} \sum_{n=1}^{\infty} [P_n(\cos t) + P_{n-1}(\cos t)] \sin n\theta = \frac{\cos \frac{1}{2}\theta H(\theta - t)}{\sqrt{\cos t - \cos \theta}}, \tag{4.14}$$

we obtain for $0 < \theta < \pi - \varepsilon$,

$$\int_0^{\theta} \frac{h_1(t)}{\sqrt{\cos t - \cos \theta}} dt + \int_0^{\pi-\varepsilon} K_{\beta}(\theta, t) h_1(t) dt = \frac{(R_2^2 - R_1^2) \theta}{2 \cos \frac{\theta}{2}}, \tag{4.15}$$

where the kernel K_β is

$$\begin{aligned}
 K_\beta(\theta, t) &= \frac{1}{\sqrt{2} \cos \frac{\theta}{2}} \sum_{n=1}^{\infty} H_n (P_n(\cos t) + P_{n-1}(\cos t)) \sin n\theta \\
 &= -2\sqrt{2}(1 + \cos t) \sin \frac{\theta}{2} \beta^2 + O(\beta^4).
 \end{aligned}
 \tag{4.16}$$

The infinite sum in Eq.(4.16) is approximated by its first term, while using the first two Legendre polynomials $P_0(x) = 1, P_1(x) = x$. Using Abel’s inversion formula applied to Eq. (4.15), we find that

$$h_1(t) - \int_0^{\pi-\varepsilon} \tilde{K}_\beta(t, s)h_1(s) ds = \frac{R_2^2 - R_1^2}{\pi} \frac{d}{dt} \int_0^t \frac{u \sin \frac{u}{2}}{\sqrt{\cos u - \cos t}} du,
 \tag{4.17}$$

where the kernel \tilde{K}_β is

$$\begin{aligned}
 \tilde{K}_\beta(t, s) &= -\frac{1}{\pi} \frac{d}{dt} \int_0^t \frac{K_\beta(u, s) \sin u}{\sqrt{\cos u - \cos t}} du \\
 &= \beta^2 \frac{2\sqrt{2}(1 + \cos s)}{\pi} \frac{d}{dt} \int_0^t \frac{\sin \frac{u}{2} \sin u}{\sqrt{\cos u - \cos t}} du + O(\beta^4).
 \end{aligned}
 \tag{4.18}$$

The substitution

$$s = \sqrt{\frac{\cos u - \cos t}{2}}
 \tag{4.19}$$

gives

$$\int_0^t \frac{\sin \frac{u}{2} \sin u}{\sqrt{\cos u - \cos t}} du = \frac{\pi}{\sqrt{2}} \sin^2 \frac{t}{2},
 \tag{4.20}$$

therefore,

$$\tilde{K}_\beta(t, s) = 2\beta^2 \cos^2 \frac{s}{2} \sin t + O(\beta^4).
 \tag{4.21}$$

Equation (4.17) is a Fredholm integral equation of the second kind for h_1 , of the form

$$(I - \tilde{K}_\beta)h = z,
 \tag{4.22}$$

where

$$z(t) = \frac{R_2^2 - R_1^2}{\pi} \frac{d}{dt} \int_0^t \frac{u \sin \frac{u}{2}}{\sqrt{\cos u - \cos t}} du.$$

Therefore, we h can be expanded as

$$h = z + \tilde{K}_{\beta z} + \tilde{K}_{\beta z}^2 + \dots, \tag{4.23}$$

which converges in L^2 . Since $c_0 = \sqrt{2}\langle h, 1 \rangle$ (Eq.(4.12)), we find an asymptotic expansion of the form

$$c_0 = \sqrt{2} [\langle z, 1 \rangle + \langle \tilde{K}_{\beta z}, 1 \rangle + \dots]. \tag{4.24}$$

The leading order term of this expansion was calculated in Ref. 5. We now estimate the error term $\langle \tilde{K}_{\beta z}, 1 \rangle$, which is also the $O(\beta^2)$ correction. Integrating by parts and changing the order of integration yields

$$\begin{aligned} \tilde{K}_{\beta z}(t) &= 2\beta^2 \frac{R_2^2 - R_1^2}{\pi} \sin t \int_0^\pi \cos^2 \frac{s}{2} ds \frac{d}{ds} \int_0^s \frac{u \sin \frac{u}{2}}{\sqrt{\cos u - \cos s}} du \\ &= \beta^2 \frac{R_2^2 - R_1^2}{\pi} \sin t \int_0^\pi \sin s ds \int_0^s \frac{u \sin \frac{u}{2}}{\sqrt{\cos u - \cos s}} du \\ &= \sqrt{2}\beta^2(R_2^2 - R_1^2) \sin t. \end{aligned} \tag{4.25}$$

Therefore,

$$\langle \tilde{K}_{\beta z}, 1 \rangle = \sqrt{2}\beta^2(R_2^2 - R_1^2) \int_0^\pi \sin t dt = 2\sqrt{2}\beta^2(R_2^2 - R_1^2). \tag{4.26}$$

We conclude that

$$c_0 = (R_2^2 - R_1^2) \left[2 \log \frac{1}{\varepsilon} + 2 \log 2 + 4\beta^2 + O(\varepsilon, \beta^4) \right]. \tag{4.27}$$

The MFPT averaged with respect to a uniform initial distribution is

$$\begin{aligned} E\tau &= \frac{c_0}{2} + \frac{1}{2} \frac{R_2^4}{R_2^2 - R_1^2} \log \frac{R_2}{R_1} - \frac{1}{4} R_2^2 \\ &= (R_2^2 - R_1^2) \left[\log \frac{1}{\varepsilon} + \log 2 + 2\beta^2 \right] \\ &\quad + \frac{1}{2} \frac{R_2^2}{1 - \beta^2} \log \frac{1}{\beta} - \frac{1}{4} R_2^2 + O(\varepsilon, \beta^4) R_2^2. \end{aligned} \tag{4.28}$$

Note that there are two different logarithmic contributions to the MFPT. The ‘‘narrow escape’’ small parameter ε contributes

$$\frac{|\Omega|_g}{\pi} \log \frac{1}{\varepsilon}, \tag{4.29}$$

as expected from the general theory (Eq. (1.1)), whereas the parameter β contributes

$$\frac{|\Omega|_g}{2\pi} \log \frac{1}{\beta}. \tag{4.30}$$

These asymptotics differ by a factor 2, because they account for different singular behaviors. The asymptotic expansion (4.29) comes out from a singular perturbation problem with singular flux near the edges, boundary layer and an outer solution, whereas the asymptotics (4.30) is an immediate result of the singularity of the Neumann function, with a regular flux.

The maximum exit time is attained at the antipode point of the center of the hole at the outer circle. Indeed, Eq. (4.7) indicates that the maximum is attained for $\theta = 0$. To determine its location along the cord $R_1 < r < R_2$, we note that $H_n \rightarrow 0$ as $\beta \rightarrow 0$. Therefore, in this limit, eqs. (4.9)-(4.10) are equivalent to the circular disk problem. The logarithmic term of Eq. (4.7) is monotonic increasing with r , and is $O(\log \frac{1}{\beta})$ for $r = R_2$. Therefore, for $\beta \ll 1$ the maximum is attained at the outer circle $r = R_2$, which is also the farthest point from the hole. Note that (4.28) is valid, with the obvious modifications, for any domain that is conformally equivalent to the annulus.

5. THE 2-SPHERE

5.1. Small Absorbing Cap

Consider a Brownian motion on the surface of a 2-sphere of radius R ⁽¹⁵⁾, described by the spherical coordinates (θ, ϕ)

$$x = R \sin \theta \cos \phi, \quad y = R \sin \theta \sin \phi, \quad z = R \cos \theta.$$

The particle is absorbed when it reaches a small spherical cap. We center the cap at the north pole, $\theta = 0$. Furthermore, the FPT to hit the spherical cap is independent of the initial angle ϕ , due to rotational symmetry. Let $v(\theta)$ be the MFPT to hit the spherical cap. Then v satisfies

$$\Delta_M v = -1, \tag{5.1}$$

where Δ_M is the Laplace-Beltrami operator ⁽¹⁵⁾ of the 2-sphere. This Laplace-Beltrami operator Δ_M replaces the regular plane Laplacian, because the diffusion occurs on a manifold [Ref. 15, and references therein]. For a function v independent of the angle ϕ the Laplace-Beltrami operator is

$$\Delta_M v = R^{-2}(v'' + \cot \theta v'). \tag{5.2}$$

The MFPT also satisfies the boundary conditions

$$v'(\pi) = 0, \quad v(\delta) = 0, \tag{5.3}$$

where δ is the opening angle of the spherical cap. The solution of the boundary value problem (5.2), (5.3) is given by

$$v(\theta) = 2R^2 \log \frac{\sin(\theta/2)}{\sin(\delta/2)}. \tag{5.4}$$

Not surprisingly, the maximum of the MFPT is attained at the point $\theta = \pi$ with the value

$$v_{\max} = v(\pi) = -2R^2 \log \sin \frac{\delta}{2} = 2R^2 \left(\log \frac{1}{\delta} + \log 2 + O(\delta^2) \right). \tag{5.5}$$

The MFPT, averaged with respect to a uniform initial distribution, is

$$\begin{aligned} E\tau &= \frac{1}{2 \cos^2 \frac{\delta}{2}} \int_{\delta}^{\pi} v(\theta) \sin \theta \, d\theta \\ &= -2R^2 \left(\frac{\log \sin(\delta/2)}{\cos^2(\delta/2)} + \frac{1}{2} \right) \\ &= 2R^2 \left(\log \frac{1}{\delta} + \log 2 - \frac{1}{2} + O(\delta^2 \log \delta) \right). \end{aligned} \tag{5.6}$$

Both the average MFPT and the maximum MFPT are

$$\tau = \frac{|\Omega|_g}{2\pi} \left(\log \frac{1}{\delta} + O(1) \right), \tag{5.7}$$

where $|\Omega|_g = 4\pi R^2$ is the area of the 2-sphere. This asymptotic expansion is the same as for the planar problem of an absorbing circle in a disk. The result is two times smaller than the result (1.1) that holds when the absorbing boundary is a small window of a reflecting boundary. The factor two difference is explained by the different local aspect angle at which the particle “sees” Ω_a , i.e. by the aspect angle explored by the trajectories. The two problems also differ in that the “narrow escape” solution is almost constant and has a boundary layer near the window, with singular fluxes near the edges, whereas in the problem of puncture hole inside a domain the flux is regular and there is no boundary layer (the solution is simply obtained by solving the ODE).

5.2. Mapping of the Riemann Sphere

We present a different approach for calculating the MFPT for the Brownian particle diffusing on a sphere. We may assume that the radius of the sphere is $1/2$, and use the stereographic projection that maps the sphere into the plane ⁽¹⁶⁾. The point $Q = (\xi, \eta, \zeta)$ on the sphere (often called the Riemann sphere)

$$\xi^2 + \eta^2 + (\zeta - 1/2)^2 = (1/2)^2$$

is projected to a plane point $P = (x, y, 0)$ by the mapping

$$x = \frac{\xi}{1 - \zeta}, \quad y = \frac{\eta}{1 - \zeta}, \quad r^2 = x^2 + y^2 = \frac{\xi^2 + \eta^2}{1 - \zeta^2}, \quad (5.8)$$

and conversely

$$\xi = \frac{x}{1 + r^2}, \quad \eta = \frac{y}{1 + r^2}, \quad \zeta = \frac{r^2}{1 + r^2}. \quad (5.9)$$

The stereographic projection is conformal and therefore transforms harmonic functions on the sphere harmonic functions in the plane, and *vice versa*. However, the stereographic projection is not an isometry. The Laplace-Beltrami operator Δ_M on the sphere is mapped onto the operator $(1 + r^2)^2 \Delta$ in the plane (Δ is the Cartesian Laplacian). The decapitated sphere is mapped onto the interior of a circle of radius

$$r_\delta = \cot \frac{\delta}{2}. \quad (5.10)$$

Therefore, the problem for the MFPT on the sphere is transformed into the planar Poisson radial problem

$$\Delta V = -\frac{1}{(1 + r^2)^2}, \quad \text{for } r < r_\delta, \quad (5.11)$$

subject to the absorbing boundary condition

$$V(r = r_\delta) = 0, \quad (5.12)$$

where

$$V(r) = v(\theta).$$

The solution of this problem is

$$V(r) = \frac{1}{4} \log \left(\frac{1 + r_\delta^2}{1 + r^2} \right). \quad (5.13)$$

Transforming back to the coordinates on the sphere, we get

$$v(\theta) = \frac{1}{2} \log \frac{\sin(\theta/2)}{\sin(\delta/2)}. \quad (5.14)$$

As the actual radius of the sphere is R rather than $1/2$, multiplying Eq. (5.14) by $(2R)^2$, we find that (5.14) is exactly (5.4).

5.3. Small Cap with an Absorbing Arc

Consider again a Brownian particle diffusing on a decapitated 2-sphere of radius $1/2$. The boundary of the spherical cap is reflecting but for a small window

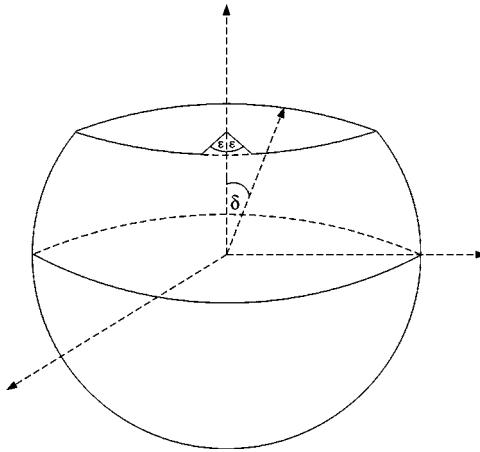


Fig. 5. A sphere of radius R without a spherical cap at the north pole of central angle δ . The particle can exit through an arc seen at angle 2ε .

that is absorbing (see Fig. 5). We calculate the mean time to absorption. Using the stereographic projection of the preceding subsection, we obtain the mixed boundary value problem

$$\begin{aligned} \Delta v &= -\frac{1}{(1+r^2)^2}, \quad \text{for } r < r_\delta, \quad 0 \leq \phi < 2\pi, \\ v(r, \phi) \Big|_{r=r_\delta} &= 0, \quad \text{for } |\phi - \pi| < \varepsilon, \\ \frac{\partial v(r, \phi)}{\partial r} \Big|_{r=r_\delta} &= 0, \quad \text{for } |\phi - \pi| > \varepsilon. \end{aligned} \tag{5.15}$$

The function

$$w(r) = \frac{1}{4} \log \left(\frac{1+r_\delta^2}{1+r^2} \right)$$

is the solution of the all absorbing boundary problem Eq.(5.13), so the function $u = v - w$ satisfies the mixed boundary value problem

$$\begin{aligned} \Delta u &= 0, \quad r < r_\delta, \quad \text{for } 0 \leq \phi < 2\pi, \\ u(r, \phi) \Big|_{r=r_\delta} &= 0, \quad \text{for } |\phi - \pi| < \varepsilon, \\ \frac{\partial u(r, \phi)}{\partial r} \Big|_{r=r_\delta} &= \frac{r_\delta}{2(1+r_\delta^2)}, \quad \text{for } |\phi - \pi| > \varepsilon. \end{aligned} \tag{5.16}$$

Scaling $\tilde{r} = r/r_\delta$, we find this mixed boundary value problem to be that of a planar disk ⁽⁵⁾, with the only difference that the constant 1/2 is now replaced by $\frac{r_\delta^2}{2(1+r_\delta^2)}$. Therefore, the solution is given by

$$a_0 = -\frac{2r_\delta^2}{1+r_\delta^2} \left[\log \frac{\varepsilon}{2} + O(\varepsilon) \right]. \quad (5.17)$$

Transforming back to the spherical coordinate system, the MFPT is

$$v(\theta, \phi) = \frac{1}{2} \log \frac{\sin \theta/2}{\sin \delta/2} - \cos^2 \frac{\delta}{2} \left[\log \frac{\varepsilon}{2} + O(\varepsilon) \right] + \sum_{n=1}^{\infty} a_n \left[\frac{\cot(\theta/2)}{\cot(\delta/2)} \right]^n \cos n\phi. \quad (5.18)$$

The MFPT, averaged over uniformly distributed initial conditions on the decapitated sphere, is

$$E\tau = -\frac{1}{2} \left(\frac{\log \sin(\delta/2)}{\cos^2(\delta/2)} + \frac{1}{2} \right) + \cos^2 \frac{\delta}{2} \left[\log \frac{2}{\varepsilon} + O(\varepsilon) \right]. \quad (5.19)$$

Scaling the radius R of the sphere into (5.19), we find that for small ε and δ the averaged MFPT is

$$E\tau = 2R^2 \left[\log \frac{1}{\delta} + 2 \log \frac{1}{\varepsilon} + 3 \log 2 - \frac{1}{2} + O(\varepsilon, \delta^2 \log \delta, \delta^2 \log \varepsilon) \right]. \quad (5.20)$$

There are two different contributions to the MFPT. The ratio ε between the absorbing arc and the entire boundary brings in a logarithmic contribution to the MFPT, which is to leading order

$$\frac{|\Omega|_g}{\pi} \log \frac{1}{\varepsilon}.$$

However, the central angle δ gives an additional logarithmic contribution, of the form

$$\frac{|\Omega|_g}{2\pi} \log \frac{1}{\delta}.$$

The factor 2 difference in the asymptotic expansions is the same as encountered in the planar annulus problem.

The MFPT for a particle initiated at the south pole $\theta = \pi$ is

$$\begin{aligned} v(\pi) &= -2R^2 \log \sin \frac{\delta}{2} - 4R^2 \cos^2 \frac{\delta}{2} \left[\log \frac{\varepsilon}{2} + O(\varepsilon) \right] \\ &= 2R^2 \left[\log \frac{1}{\delta} + 2 \log \frac{1}{\varepsilon} + 3 \log 2 + O(\varepsilon, \delta^2 \log \delta, \delta^2 \log \varepsilon) \right]. \end{aligned} \quad (5.21)$$

We also find the location (θ, ϕ) for which the MFPT is maximal. The stationarity condition $\frac{\partial v}{\partial \phi} = 0$ implies that $\phi = 0$, as expected (the opposite ϕ -direction to the center of the window). The infinite sum in Eq. (5.18) is $O(1)$. Therefore, for $\delta \ll 1$, the MFPT is maximal near the south pole $\theta = \pi$. However, for $\delta = O(1)$, the location of the maximal MFPT is more complex.

Finally, we remark that the stereographic projection also leads to the determination of the MFPT for diffusion on a 2-sphere with a small hole as discussed above, and an all reflecting spherical cap at the south pole. In this case, the image for the stereographic projection is the annulus, a problem solved in Section 4

ACKNOWLEDGMENTS

This research was partially supported by research grants from the Israel Science Foundation, US-Israel Binational Science Foundation, and the NIH Grant No. UPSHS 5 RO1 GM 067241. D. H. is incumbent to the Madeleine Haas Russell Career Development Chair, his research is partially supported by the program “Chaire d’Excellence.” The authors thank R.S. Eisenberg for critical review of the manuscript.

REFERENCES

1. B. Hille, *Ionic Channels of Excitable Membranes*, 2nd ed., (Sinauer, Mass., 1992).
2. D. Holcman and Z. Schuss, Escape through a small opening: receptor trafficking in a synaptic membrane. *J. Stat. Phys.* **117**(5–6):975–1014 (2004).
3. A. J. Borgdorff and D. Choquet, Regulation of AMPA receptor lateral movements. *Nature* **417**(6889):649–653 (2002).
4. A. Singer, Z. Schuss, D. Holcman and R. S. Eisenberg, Narrow Escape, Part I, (this journal).
5. A. Singer, Z. Schuss and D. Holcman, Narrow Escape, part II: The circular disk. (this journal).
6. I. N. Sneddon, *Mixed Boundary Value Problems in Potential Theory*, (Wiley, NY, 1966).
7. V. I. Fabrikant, *Applications of Potential Theory in Mechanics*, (Kluwer, 1989).
8. V. I. Fabrikant, *Mixed Boundary Value Problems of Potential Theory and Their Applications in Engineering*, (Kluwer, 1991).
9. H. P. McKean, Jr., *Stochastic Integrals*, (Academic Press, NY, 1969).
10. Z. Schuss, *Theory and Applications of Stochastic Differential Equations*, (Wiley Series in Probability and Statistics, Wiley, NY 1980).
11. P. R. Garabedian, *Partial Differential Equations*, (Wiley, NY 1964).
12. V.A. Kozlov, V.G. Mazya and J. Rossmann, *Elliptic Boundary Value Problems in Domains with Point Singularities*, American Mathematical Society, Mathematical Surveys and Monographs, vol. 52, (1997).
13. W. D. Collins, On some dual series equations and their application to electrostatic problems for spheroidal caps, *Proc. Cambridge Phil. Soc.* **57**:367–384 (1961).
14. W.D. Collins, “Note on an electrified circular disk situated inside an earthed coaxial infinite hollow cylinder”, *Proc. Cambridge Phil. Soc.* **57**:623–627 (1961).
15. B. Øksendal, *Stochastic Differential Equations*, 5th ed., (Springer, Berlin Heidelberg, 1998).
16. E. Hille, *Analytic Function Theory*, vol. 1, (Chelsea Publishing Company, New York, 1976).